Leucine retention in lysosomes is regulated by starvation

Urmi Bandyopadhyay[a,1], Pavlina Todorova[a], Natalya N. Pavlova[b], Yuma Tada[a], Craig B. Thompson[b,c,1], Lydia W.S. Finley[a,c], and Michael Overholtzer[a,c,1]

[a]Cell Biology Program, Memorial Sloan Kettering Cancer Center, New York, NY 10065; [b]Cancer Biology and Genetics Program, Memorial Sloan Kettering Cancer Center, New York, NY 10065; and [c]Louis V. Gerstner Jr. Graduate School of Biomedical Sciences, Memorial Sloan Kettering Cancer Center, New York, NY 10065

Contributed by Craig B. Thompson; received August 13, 2021; accepted December 27, 2021; reviewed by Eric Baehrecke and Jayanta Debnath

Cells acquire essential nutrients from the environment and utilize adaptive mechanisms to survive when nutrients are scarce. How nutrients are trafficked and compartmentalized within cells and whether they are stored in response to stress remain poorly understood. Here, we investigate amino acid trafficking and uncover evidence for the lysosomal transit of numerous essential amino acids. We find that starvation induces the lysosomal retention of leucine in a manner requiring RAG-GTPases and the lysosomal protein complex Ragulator, but that this process occurs independently of mechanistic target of rapamycin complex 1 activity. We further find that stored leucine is utilized in protein synthesis and that inhibition of protein synthesis releases lysosomal stores. These findings identify a regulated starvation response that involves the lysosomal storage of leucine.

lysosome | leucine | mTOR

Mammalian cells can sense the availability of essential nutrients and integrate these signals into decisions to grow and divide (1). For example, numerous mechanisms detect the presence of amino acids or other metabolites and relay signals to the mechanistic target of rapamycin complex 1 (mTORC1) protein kinase complex, which in turn increases the rates of anabolic processes to allow cells to grow when nutrients are available (2–4). Conversely when nutrients are scarce, cells respond by up-regulating catabolic processes that recycle essential nutrients in support of cell survival (5). While numerous signaling mechanisms that allow cells to sense and respond to nutrients have been described (6), how nutrients themselves are trafficked and potentially compartmentalized within cells remains poorly understood. Here, we developed a method to study the trafficking of amino acids using intact cells and use it to identify a storage mechanism that is regulated in response to starvation.

Results

To study amino acid trafficking, a classical long-term protein degradation assay (7, 8) was modified to quantify the short-term movements of ^{3}H-labeled amino acids added to cells at 1/1,000th the normal concentration (Fig. 1*A*). Following a 15-min pulse with radioactive amino acid and then chase with nonradiolabeled amino acid, 70 to 80% of ^{3}H-leucine was retained in cells, while 20 to 30% was recycled to the medium after 1 h (Fig. 1*B*), a pattern observed with numerous cell types (*SI Appendix*, Fig. S1 *A–E*). While the rapid equilibration of amino acids has been observed previously (8), we noticed that when cells were cultured in the absence of exogenous leucine during the chase, the fraction of ^{3}H-leucine that was normally released from cells was instead retained, suggesting the presence of a regulated process (Fig. 1*C*). Two lysosome-damaging agents, L-leucyl-L-leucine methyl ester (LLOMe [9]) and glycyl-L-phenylalanine-β-naphthylamide (GPN [10]), were identified as potent inhibitors of the ability of starved cells to retain leucine, an effect that was also observed in numerous cell types (Fig. 1 *C* and *D* and *SI Appendix*, Figs. S1 and S2), suggesting that leucine might be retained within lysosomes during starvation (11). Consistent with this, lysosomes purified through gradient centrifugation (12) or an immunopurification method called LysoIP (*SI Appendix*, Fig. S3) (13) contained more ^{3}H-leucine when isolated from starved cells than from fed cells in a manner that was reversed by treatment with LLOMe, demonstrating that starved cells can store leucine within lysosomes (Fig. 1 *E* and *F*). We further found that treatment of cells with LLOMe even after a 1- or 2-h delay still led to significant ^{3}H-leucine release, demonstrating that starved cells can store leucine in lysosomes for prolonged periods (Fig. 1*G*).

While treatment with LLOMe led to ^{3}H-leucine release from starved cells, there was only a minor effect when cells were cultured in full medium (Fig. 1*C*), suggesting either that ^{3}H-leucine did not transit lysosomes under nutrient-replete conditions or that it transited more rapidly than LLOMe-induced lysosome rupture, which occurred after 15 min, as detected by the green fluorescent protein (GFP)–galectin-3 reporter that binds to ruptured lysosomes (Fig. 1*D* and *SI Appendix*, Fig. S2) (11). When cells were pretreated with LLOMe (added in both the pulse and the chase), a strong effect was observed, as more than 80% of ^{3}H-leucine was released from cells under nutrient-replete conditions (Fig. 1*H*),

Significance

Cells can respond to starvation by up-regulating stress responses that promote the recycling or scavenging of essential nutrients. We identify a starvation response that allows cells to store the essential amino acid leucine within lysosomes when extracellular amino acids are scarce. This "storage" response allows cells to sequester an essential amino acid in support of protein synthesis. We find that numerous essential amino acids are trafficked through lysosomes even when extracellular concentrations are high, suggesting that constitutive flux through lysosomes is related to starvation-induced storage.

Author contributions: U.B., C.B.T., L.W.S.F., and M.O. designed research; U.B., P.T., and N.N.P. performed research; P.T., N.N.P., and Y.T. contributed new reagents/analytic tools; U.B. analyzed data; U.B. and M.O. wrote the paper; and C.B.T., L.W.S.F., and M.O. oversaw project administration.

Reviewers: E.B., University of Massachusetts Medical School; J.D., University of California, San Francisco.

Competing interest statement: C.B.T. is a founder of Agios Pharmaceuticals and a member of its scientific advisory board. Memorial Sloan Kettering Cancer Center and one investigator involved in this study (M.O.) have financial interests in Elucida Oncology.

See online for related content such as Commentaries.

[1]To whom correspondence may be addressed. Email: thompsonc@mskcc.org, overhom1@mskcc.org, or bandyopu@mskcc.org.

This article contains supporting information online at http://www.pnas.org/lookup/suppl/doi:10.1073/pnas.2114912119/-/DCSupplemental.

Published February 1, 2022.

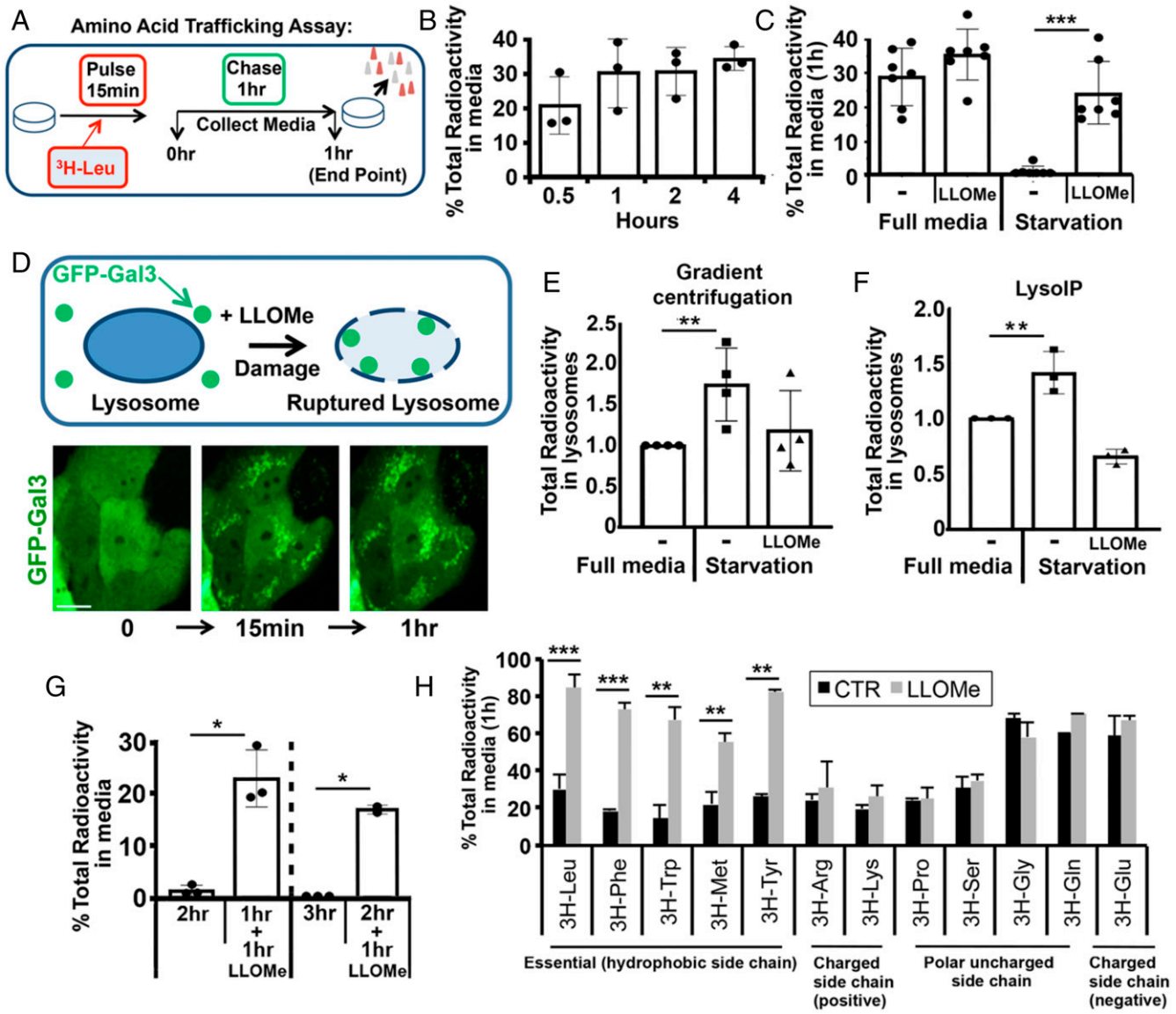

Fig. 1. Leucine is retained in starved cells and released upon lysosome rupture. (*A*) Amino acid trafficking assay involving pulse labeling with ^{3}H-labeled amino acid (e.g., ^{3}H-leucine) for 15 min, followed by a 1-h or longer chase in the presence or absence of nonradiolabeled amino acids. ^{3}H-Labeled amino acids released or remaining in cells at the end of the chase are quantified and added together for the total. (*B*) Percent ^{3}H-leucine released from MEFs at different time points. (*C*) Percent ^{3}H-leucine released in the presence or absence of amino acids, with or without LLOMe added in the 1-h chase (MEFs). (*D*) GFP–galectin-3 (GFP–Gal3) accumulates in damaged lysosomes ruptured with LLOMe after 15 min. (Scale bar = 10 μm.) See *SI Appendix*, Fig. S2. (*E* and *F*) ^{3}H-Leucine in lysosomes isolated from cells cultured under nutrient-replete or leucine-starved conditions in the presence or absence of LLOMe in the 1-h chase. Lysosomes were isolated through gradient centrifugation from MEFs (*E*) or by LysoIP from HEK-293T cells (*F*). Total ^{3}H-leucine counts from lysosomal fractions were normalized to the amount of Lamp1 protein in each prep quantified by Western blotting (see *SI Appendix*, Fig. S3). (*G*) Percent ^{3}H-leucine released after 1-h and 2-h starvation periods followed by 1 h of LLOMe treatment. (*H*) Percent ^{3}H-amino acids released in full medium after 1 h in the presence or absence of LLOMe added during the pulse and chase. Different amino acid classes are labeled. For all graphs, individual data points represent means from at least three independent biological replicates performed in triplicate. Bars show means from all biological replicates, and error bars show standard deviation (SD).

suggesting that leucine transits lysosomes in fed cells but at a faster rate than during starvation. To examine the trafficking of other amino acids, cells were treated with additional tracers in the presence or absence of LLOMe. Most of the essential, hydrophobic side chain-containing amino acids (EAA) (phenylalanine, tryptophan, methionine, and the conditionally essential amino acid tyrosine) were released when cells were treated with LLOMe, consistent with trafficking through lysosomes, whereas nonessential, charged, and polar side chain-containing amino acids (NAA) were unaffected by LLOMe, consistent with a lysosome-independent itinerary (Fig. 1*H*).

To examine the fate of stored amino acids, we first sought to investigate the relationship between lysosome storage and messenger RNA (mRNA) translation. When starved cells were treated with cycloheximide (CHX), an inhibitor of translation elongation, or leucinol, a nonfunctional leucine derivative that inhibits leucyl transfer RNA (tRNA) charging, ^{3}H-leucine was released to a similar extent as in response to LLOMe (Fig. 2*A*). LLOMe and CHX both inhibited the incorporation of ^{3}H-leucine into protein in starved cells and did not have an additive effect when combined (Fig. 2*B*), suggesting that the inhibition of protein synthesis leads to the emptying of lysosomal stores. When cells were treated with CHX under nutrient-replete conditions, no effect on ^{3}H-leucine trafficking was observed unless cells were pretreated during the pulse (*SI Appendix*, Fig. S4 *A* and *B*), suggesting that the movement of ^{3}H-leucine through

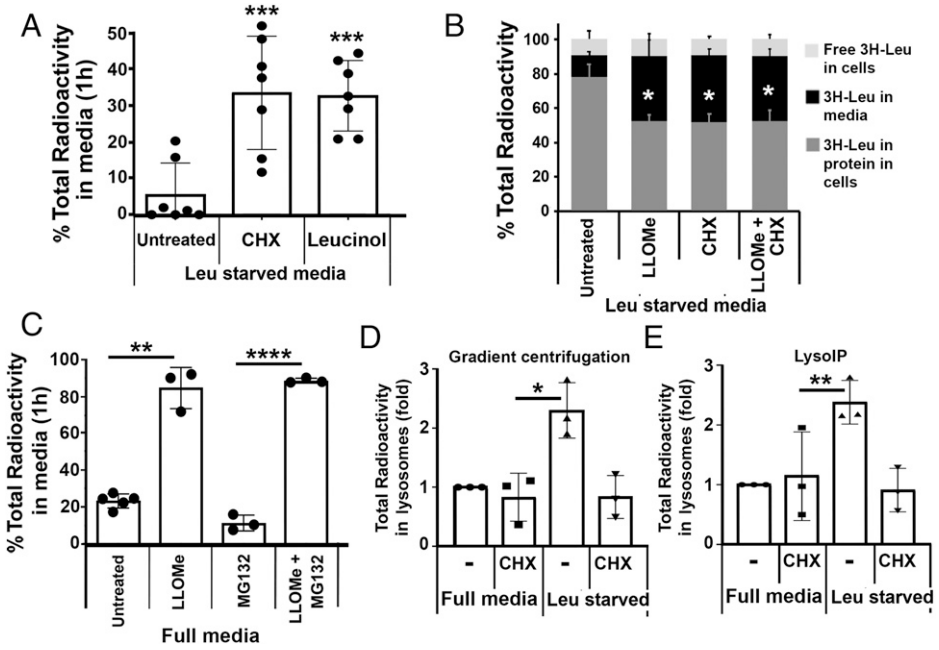

Fig. 2. Relationship between lysosomal storage and protein synthesis. (*A*) Percent ^{3}H-leucine released from MEFs in starvation medium in the presence or absence of CHX or leucinol during the chase. (*B*) Percent ^{3}H-leucine entering mRNA translation (gray bar), released (black bar), or retained in cells as free amino acid (light gray bar) in the presence or absence of LLOMe and CHX in the chase. (*C*) Percent ^{3}H-leucine released from MEFs in the presence or absence of MG132 or LLOMe added in the pulse and chase in full medium. (*D* and *E*) ^{3}H-leucine content of lysosomes isolated from MEFs (*D*) or HEK-293T cells (*E*) in the presence or absence of leucine and CHX by gradient centrifugation-based lysosomal purification (*D*) or by LysoIP (*E*). Data are expressed as fold change ^{3}H-leucine normalized by Lamp1 immunoblotting from each prep. For all graphs, individual data points represent means from at least three independent biological replicates performed in triplicate. Bars show means from all biological replicates, and error bars show SD.

lysosomes and utilization in protein synthesis occurs with faster kinetics under fed conditions. We also treated cells with the proteasome inhibitor MG132 in the presence or absence of LLOMe and found that while MG132 treatment modestly reduced the amount of ^{3}H-leucine that was released from cells in full medium, it had no effect when lysosomes were ruptured with LLOMe, consistent with lysosomal leucine transit occurring upstream of protein synthesis and subsequent proteasomal degradation (Fig. 2*C*). To further examine the relationship between protein synthesis and lysosomal storage, ^{3}H-leucine was quantified in lysosomes purified from cells under nutrient-replete or starved conditions in the presence and absence of CHX. While starvation increased the amount of ^{3}H-leucine retained in purified lysosomes, treatment with CHX inhibited this effect (Fig. 2 *D* and *E*).

To identify additional regulators of lysosome storage, we first examined the mTORC1 kinase that is reported to regulate the export of amino acids from lysosomes (14). Inhibition of mTOR by treatment with Torin1 (15) did not mimic the effect of starvation, as it did not lead to retention of the ^{3}H-leucine tracer in lysosomes when added to cells in full medium (Fig. 3*A* and *SI Appendix*, Fig. S4*A*). When cells were pretreated with Torin1 (during the pulse), a small but reproducible increase in the release of ^{3}H-leucine from cells was observed, demonstrating that while mTOR inhibition does not lead to storage, it can induce a partial release of the tracer in a manner similar to, but to a lesser extent than, treatment with CHX (*SI Appendix*, Fig. S4*B*). We further examined if mTOR might regulate starvation-induced ^{3}H-leucine retention but observed no effects on the storage of ^{3}H-leucine when examined with intact cells or in purified lysosomes, suggesting that starvation-induced lysosome storage can be regulated independently of mTOR (Fig. 3 *B*–*F*). Further investigation of the mTORC1 pathway through knockout (KO) of *Depdc5*, which encodes a component of the Gator1 complex that inhibits mTORC1 during leucine starvation (16), knockdown of *SESTRIN2*, which blocks leucine sensing by mTORC1 (17), or KO of tuberous sclerosis 2 (*Tsc2*), which also leads to constitutive mTORC1 activity (18), revealed no significant effects or only minor effects (in the case of *SESTRIN2* knockdown) on leucine storage (Fig. 3 *F* and *G* and *SI Appendix*, Fig. S4*C*), demonstrating overall that starved cells can store leucine within lysosomes in a manner that can be regulated independently of mTORC1.

Although mTOR did not regulate leucine storage, we examined a potential role for RAG-GTPases that participate in forming an mTORC1-regulating complex that is scaffolded to the lysosomal membrane (19). While the deletion of *RagA* and *RagB* had no effect under nutrient-replete conditions, the loss of *RagA*/*B* inhibited the storage of leucine in starved cells (Fig. 4*A*). Lysosomes purified from *RagA*/*B*-KO cells also showed no increased in ^{3}H-leucine in response to starvation (*SI Appendix*, Fig. S5*A*). We also examined the effect of deleting genes that encode proteins constituting part of a complex called Ragulator (19), which binds and activates RAG-GTPases at the lysosomal membrane, including *Lamtor1* and *Lamtor2* (late endosomal/lysosomal adaptor mTOR activator 1 and 2). Similar to the loss of *RagA*/*B*, *Lamtor1*, or *Lamtor2* deletion inhibited starvation-induced storage (Fig. 4 *B* and *C*) and, like treatment with LLOMe or CHX, inhibited the incorporation of ^{3}H-leucine into protein in starved cells. Treatment with Torin1, by contrast, had no effect (Fig. 4*D*). Together, these data demonstrate that RAGA/B and LAMTOR1/2 can control the storage of leucine in lysosomes in an apparently mTORC1-independent manner.

While the majority of cells we examined were able to store leucine in response to starvation, we identified one cancer cell line, MCF7 breast cancer cells, that was largely unable to store, as more than 50% was still released from starved cells (Fig. 4*E*). Nearly 70% of the tracer was also released from MCF7 cells under nutrient-replete conditions, suggesting a low relative rate of amino acid utilization (Fig. 4*F*). We found that MCF7

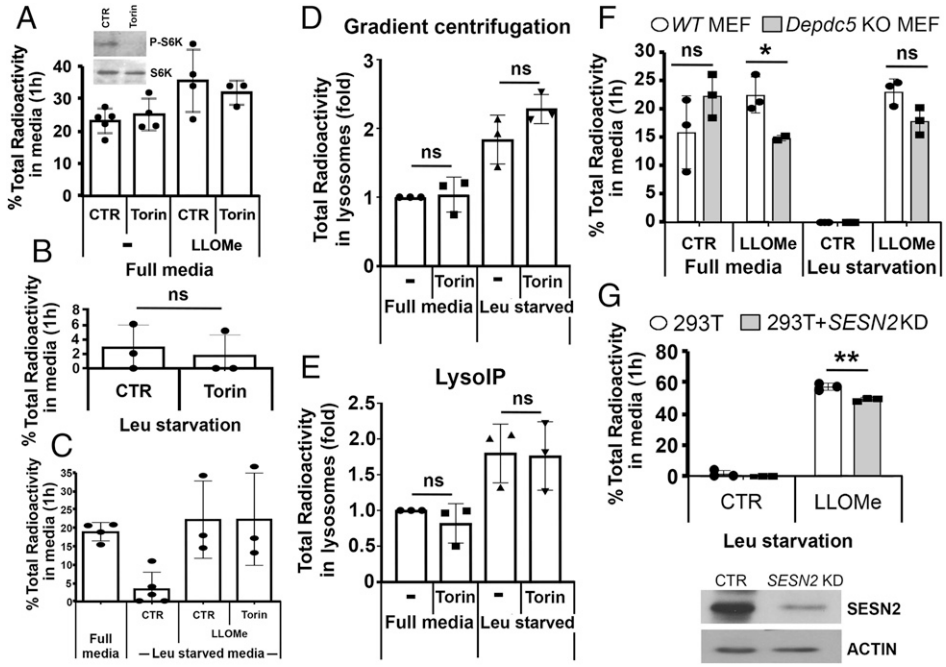

Fig. 3. Leucine storage is mTOR independent. (*A*) Percent ^{3}H-leucine released from MEFs in the presence or absence of Torin1 in nutrient-replete medium with or without LLOMe added in the chase. Western blot shows inhibition of mTOR activity in response to Torin1; CTR, control. (*B*) Percent ^{3}H-leucine released by MEFs into leucine-free medium in the presence or absence of Torin1 added to the pulse and chase; ns shows lack of significance between control and LLOMe. (*C*) Percent ^{3}H-leucine released from MEFs cultured in nutrient-replete or leucine-free medium in the presence or absence of Torin1 (added in the pulse and chase) and LLOMe (added in the chase). (*D* and *E*) ^{3}H-Leucine content of lysosomes isolated after 1 h in the presence and absence of leucine, with or without Torin1, by gradient centrifugation from MEFs (*D*) or by LysoIP from HEK-293T cells (*E*). Total ^{3}H-leucine from lysosomal fractions normalized to Lamp1 protein quantified by Western blotting. (*F*) Percent ^{3}H-leucine released from wild-type (*wt*) or *Depdc5*-KO MEFs in nutrient-replete or leucine-free medium in the presence or absence of LLOMe in the chase. (*G*) Percent ^{3}H-leucine released from control and *SESTRIN2*-knockdown HEK-293T cells in the presence or absence of LLOMe added in the chase. For all graphs, individual data points represent means from at least three independent biological replicates performed in triplicate. Bars show means from all biological replicates, and error bars show SD.

cells expressed low levels of RagA and RagB proteins (Fig. 4*G*) and that RagA/B overexpression could restore leucine storage in response to starvation in an LLOMe-inhibitable manner (Fig. 4*E* and *SI Appendix*, Fig. S5*B*). RagA/B overexpression also reduced the fraction of ^{3}H-leucine that was released under nutrient-replete conditions in a manner unaffected by LLOMe and significantly increased the rate of protein synthesis (Fig. 4*F* and *SI Appendix*, Fig. S5*C*). These data demonstrate that the expression of RagA/B proteins regulates the ability of starved cells to store amino acids in lysosomes and contributes to determining the setpoint of amino acid utilization in protein synthesis under nutrient-replete conditions.

Discussion

Taken together our findings show that starved cells can store leucine within lysosomes in a RAGA/B- and LAMTOR1/2-dependent, mTORC1-independent manner, and that lysosomal stores of leucine are utilized in protein synthesis (Fig. 4*H*). The lysosomal import and export of amino acids is emerging as an important trafficking activity that is linked to the ability of mammalian cells to sense essential nutrients (14, 20). The amino acids shown here to transit lysosomes relate closely to those from a recent report identifying lysosomal amino acid pools by mass spectrometry of purified organelles, where seven amino acids (leucine, valine, isoleucine, tyrosine, phenylalanine, methionine, and tryptophan) were shown to be exported from lysosomes in an mTORC1-dependent manner (14). The five amino acids found here to transit lysosomes fit into this group (Fig. 1*H*), providing further evidence that these amino acids are associated with lysosomal transport. Our findings demonstrate that lysosomal storage also occurs as a regulated response to starvation. While we identified regulation of lysosomal leucine storage by the Rag/Ragulator complex, we did not find evidence for regulation by mTORC1, which differs from measurements made through mass spectrometry-based analysis of purified organelles (14). One difference may be that our method measures the relative flux rate of a pulsed tracer through cells or lysosomes rather than measuring the total amounts of amino acids within intracellular or lysosomal pools.

The mechanisms underlying how the Rag/Ragulator complex contribute to controlling amino acid storage will be important to identify. We find that activity of the mitogen-activated protein kinase/extracellular signal-regulated kinase (MAPK/ERK) kinase (MEK), which can bind to Ragulator (21), is not involved, and lysosomal acidification as well as activity of the autophagy pathway, which are reported to be disrupted in *RagA/B*-KO cells (22), are also not required for the lysosomal trafficking or storage of leucine (*SI Appendix*, Fig. S6). Whether autophagy-related genes other than *Atg5* examined here could potentially be involved in regulating leucine storage awaits further investigation. Future studies may also reveal which amino acid transporter proteins, including those previously implicated in mediating leucine trafficking at lysosomes (e.g., SLC38A9, SLC1A5, and SLC7A5–SLC3A2 [LAT1]), may be involved in the regulation of starvation-induced lysosomal storage that we observe (13, 20, 23). We find that the inhibition of protein synthesis by treatment with CHX or leucinol leads to release of stored ^{3}H-leucine, a result that could conceivably be linked to the reduced expression of protein(s) that regulate lysosome storage. Alternatively, this may be a consequence of increased intracellular pools of free amino acids that accumulate when translation is blocked. It is possible that the partial release of

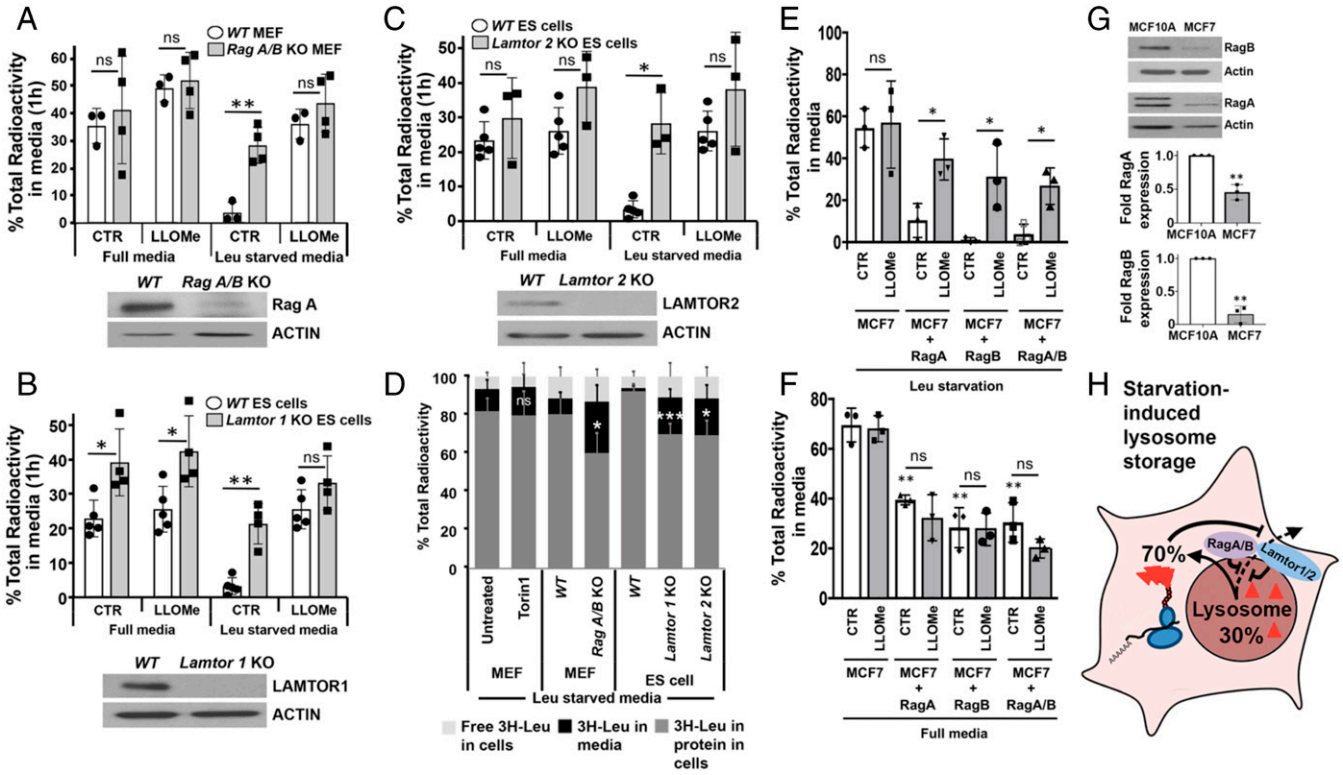

Fig. 4. RAG-GTPases and LAMTOR proteins are required for lysosomal leucine storage. (*A–C*) Percent ^{3}H-leucine released from *wt* and *RagA/B*-KO MEFs or *wt* and *Lamtor1* or *Lamtor2*-KO ESCs in nutrient-replete or leucine-free medium in the presence or absence of LLOMe in the chase. Western blots show loss of expression of RAGA, LAMTOR1, and LAMTOR2 in KO cells. (*D*) Distribution of ^{3}H-leucine in *wt* and different KO MEFs or Torin1-treated MEFs entering protein synthesis (gray bars), released (black bars), or retained in cells as free amino acid (light gray bars). (*E* and *F*) Percent ^{3}H-leucine released from control or *RagA*- or *RagB*- overexpressing MCF7 cells in leucine-free (*E*) or nutrient-replete (*F*) medium in the presence or absence of LLOMe in the chase. Asterisks in (*F*) show statistical significance compared to control; ns shows lack of significance between control and LLOMe. (*G*) Expression levels of RagA and RagB proteins in MCF7 cells compared to MCF10A cells. See also *SI Appendix*, Fig. S5*B*. Individual data points in (*A–F*) represent means from at least three independent biological replicates performed in triplicate. Bars show means from all biological replicates, and error bars show SD. (*H*) Model: essential amino acids, including leucine, transit the lysosome and are utilized in protein synthesis. Excess amino acid is released into the medium (dashed arrow). Under starvation conditions, leucine is retained in lysosomes in a *RAGA/B*- and *LAMTOR1/2*-dependent manner and utilized for protein synthesis. The inhibition of protein synthesis releases lysosomal stores.

^{3}H-leucine in response to mTOR inhibition, which also reduces protein synthesis, could relate to this effect as well.

The discovery that starvation induces the regulated lysosomal retention of leucine provides additional evidence, along with a previous study (14), that mammalian lysosomes act as nutrient storage organelles. Our study utilized a newly developed method to trace amino trafficking with intact cells in addition to a lysosome purification strategy that was previously published (13). Additional studies, potentially employing new methodology, will be needed to decipher how lysosome storage mechanisms may function at physiologic nutrient concentrations and within intact tissues. In yeast, the lysosome-like vacuole functions as a storage organelle for free amino acids, in particular neutral and basic amino acids whose concentrations in the vacuole increase during cell growth to support protein synthesis by acting as a buffer against extracellular fluctuations (24). Cancer cells in nutrient-deprived microenvironments are known to up-regulate autophagy and macropinocytosis to recycle or scavenge free amino acids through the lysosomal digestion of proteins (5, 25). Macropinocytic ingestion of albumin from the extracellular environment has been shown to generate enough free leucine, the most abundant amino acid in the mammalian proteome and also in albumin, to activate mTORC1 activity and support cell growth in the absence of exogenous leucine (26). Our findings reveal that starving mammalian cells sequester free leucine within lysosomes, and this pool is utilized in protein synthesis, consistent with lysosomes acting as a storage organelle in support of protein synthesis when extracellular concentrations are reduced. Intriguingly, while many different cell types we examined showed the ability to store ^{3}H-leucine in response to starvation, we also identified MCF7 breast cancer cells as defective for starvation-induced storage, suggesting that some cancer cells may modulate storage capacity in complex ways. The potential roles of lysosome storage in supporting tumorigenic growth will be important to investigate.

Materials and Methods

Cell Culture. All mammalian cell lines were cultured at 5% CO_2 and 37 °C. Mouse embryo fibroblasts (MEFs), HEK-293T cells, and RAW 264.7 mouse macrophages were cultured in high-glucose Dulbecco's minimum essential medium (DMEM) supplemented with 10% fetal bovine serum (FBS). *RagA/B*-KO MEFs were generated by treating *RagA/B* wild-type (WT) MEFs with 1 μM tamoxifen in DMEM supplemented with 10% FBS for 3 to 4 d (22). MCF10A human mammary epithelial cells were cultured in 1:1 DMEM and Ham's F-12 (DMEM-F12) supplemented with 10% horse serum (HS), epidermal growth factor (EGF), insulin, and cholera toxin, as previously described (27). Mouse embryonic stem cell (ESC) lines were previously derived from C57BL/6 × 129S4/SvJae F1 male embryos (28). ESCs were maintained in KnockOut DMEM (Gibco) supplemented with 10% FBS (Gemini), 0.1 mM 2-mercaptoethanol, 2 mM L-glutamine, and 1,000 U/mL leukemia inhibitory factor (LIF; Gemini). For all radiolabeled amino acid trafficking assays, mouse ESCs grown in maintenance medium were metabolically radiolabeled with 2 μCi/mL ^{3}H-leucine at 37 °C for 15 min. Labeled cells were washed three times with phosphate-buffered saline (PBS) and incubated in experimental medium containing a 1:1 mix of leucine- and glutamine-free DMEM and Neurobasal medium

(generated in-house) supplemented with 10% dialyzed FBS (Gemini) and 4 mM glutamine with or without 0.8 mM leucine. All amino acid-free medium was supplemented with 10% dialyzed FBS or HS. Cells expressing GFP–galectin-3 were generated by retroviral transduction following generation of viral particles in HEK-293T cells using a GFP–galectin-3 construct acquired from Addgene (plasmid number 73080).

Reagents. Cells were treated with 10 μM MG132 (Sigma, St. Louis, MO), 1 μM Torin1 (Tocris Bioscience, Bristol, UK), 10 μg/mL CHX (Sigma, St. Louis, MO), 5 mM leucinol (Sigma, St. Louis, MO), 1 μM tamoxifen (Sigma, St. Louis, MO), 100 nM concanamycin A, and 1 μM GSK212 (MEK inhibitor) as indicated. For experiments under starvation conditions, cells were treated with the lysosome-damaging agent LLOMe (Cayman Chemical, Ann Arbor, MI) at 300 nM for 1 h during the chase period, following the 15-min ^{3}H-leucine pulse. For experiments in nutrient-replete medium, 300 nM LLOMe was added in both the pulse and chase periods, unless indicated otherwise. HEK-293T cells were treated with the lysosome-damaging agent GPN (Cayman Chemical, Ann Arbor, MI) at 400 μM in the chase period. For LysoTracker staining experiments, MEFs were incubated with 100 nM LysoTracker Red DND-99 (L7528, Thermo Fisher Scientific, Waltham, MA) for 10 min followed by three PBS washes before treatment with or without 100 nM concanamycin A. Cells were then imaged by confocal microscopy. The following antibodies were used: anti-RagA (4357, Cell Signaling, Danvers, MA), anti-Lamtor1 (8975, Cell Signaling), anti-Lamtor2 (8145, Cell Signaling), anti-human Lamp1/CD107a (H4A3) (555798, BD Biosciences, San Jose, CA), anti-mouse Lamp1/CD107a (1D4B) (553792, BD Biosciences, San Jose, CA), anti-Sesn2 (10795-1-AP, Proteintech, Rosemont, IL), anti-P-S6K (9234, Cell Signaling, Danvers, MA), anti-S6K (9202, Cell Signaling, Danvers, MA), anti-VDAC1 (4866, Cell Signaling, Danvers, MA), anti-Pex13 (ABC143, Millipore Sigma, Burlington, MA), anti-GM130 (610822, BD Biosciences, San Jose, CA), anti-puromycin (12D10) (MABE343, Millipore Sigma, Burlington, MA), anti-actin (ab14128, Abcam, Cambridge, MA), and anti-Flag M2 affinity gel (A2220, Millipore Sigma, Burlington, MA), anti-P-Erk1/2 (Thr202/Tyr204) (9101, Cell Signaling, Danvers, MA), and anti-Erk1/2 (9102, Cell Signaling, Danvers, MA).

Radioactive Isotopes. ^{3}H-Leucine (leucine, L-[4,5-^{3}H]), ^{3}H-phenylalanine (phenylalanine, L-[2,3,4,5,6-^{3}H]), ^{3}H-tryptophan (tryptophan, L-[5-3H(N)]), ^{3}H-methionine (L-[methyl-^{3}H]-methionine), ^{3}H-tyrosine (L-[ring-3,5-^{3}H]-tyrosine), ^{3}H-arginine (arginine monohydrochloride L-[2,3,4-^{3}H]-arginine), ^{3}H-lysine (L-[4,5-^{3}H(N)]-lysine), ^{3}H-proline (L-[2,3,4,5-^{3}H]-proline), ^{3}H-serine (L-[^{3}H(G)]-serine), ^{3}H-glycine (glycine, [2-^{3}H]-glycine), ^{3}H-glutamine (L-[3,4-^{3}H(N)]-glutamine), and ^{3}H-glutamic acid (L-[3,4-^{3}H]-glutamic acid) are from PerkinElmer (Waltham, MA).

Radiolabeled Amino Acid Trafficking Assay. To measure amino acid trafficking, 0.2×10^6 to 0.4×10^6 cells per well in 12-well plates were metabolically radiolabeled with 2 μCi/mL ^{3}H-leucine in 500 μL of full medium at 37 °C for 15 mins, followed by triple washing in PBS and incubating in growth medium for a chase in the presence or absence of the indicated amino acids. Medium was then collected at different time intervals to monitor the presence of trichloroacetic acid (TCA)-soluble radioactivity. Collected medium was precipitated with 20% TCA and 2 mg/mL bovine serum albumin (BSA) by incubating at 4 °C overnight. To separate the soluble fraction containing free amino acids or small peptides from the precipitated fraction containing proteins, filtration was performed using a Millipore vacuum manifold, and the filtrate was then measured in a TRI-CARB 4910TR Liquid Scintillation Counter (from PerkinElmer) to obtain the absolute value of ^{3}H-leucine in dissociation per minute (DPM). The total radioactivity incorporated into cells was determined as the amount of radioactivity in labeled cells immediately after washing at the end of the last time point of the chase, which was recovered by solubilizing the cells in 1 mL of 0.1 N NaOH and 0.1% sodium deoxycholate at 37 °C overnight. The total amount of radioactive amino acid uptake by cells during the pulse labeling was measured by calculating the radioactivity present within cells at the end of the chase period along with the radioactivity present in the medium (29, 30). Exported radiolabeled ^{3}H-leucine in the medium during the chase was expressed as the percentage of total (cell lysate plus medium) uptake. The timing of drug treatments in the protocol for each experiment is indicated in each figure legend. To quantify the incorporation of radiolabeled leucine (^{3}H-leucine) in intracellular proteins, the amount of TCA-precipitable radioactivity in the cell lysate was measured following three PBS washes and solubilization in 0.1 N NaOH and 0.1% sodium deoxycholate at 37 °C overnight.

Radiolabeling of Cells Prior to Subcellular Fractionation/Lysosome Isolation. Cells were pulse labeled with radioactive ^{3}H-leucine for 15 min, which were then washed thoroughly with 1× PBS three times, followed by a 1-h-long chase in nonradioactive medium supplemented with or without leucine and different pharmacological agents, as indicated, prior to subcellular fractionation, leading to lysosome or endolysosomal compartment isolation.

Subcellular Fractionation: Isolation of Lysosomes from Cells in Culture. Lysosomes from cultured cells were isolated from mitochondria–lysosomal fractions by centrifugation through metrizamide/Percoll discontinuous gradients (12). Briefly, confluent cells (100×10^6) were plated in 150 mm × 25 mm dishes (Corning, NY, USA) and were maintained in medium supplemented with or without leucine in the presence and absence of pharmacological agents, as indicated, prior to lysosome isolation. Cells were washed thoroughly with cold PBS twice and collected by centrifuging at 500 × *g* for 5 min at 4 °C in a Sorvall RC6 Plus centrifuge (SS34 rotor) and then further washed with 0.25 M sucrose, pH 7.2, and pelleted in a similar manner. Upon resuspending the cell pellet in 1.5 mL of 0.25 M sucrose, cell membranes and nuclear membranes were disrupted, retaining the integrity of lysosomal membranes, using a nitrogen cavitation chamber (35 psi for 7 min) (Parr Instrument Company, Moline, IL). After cavitation, complete cell breakage was ensured by homogenization with 10 strokes using a Teflon/glass homogenizer. The cell lysate was then subjected to centrifugation at 2,500 × *g* for 15 min at 4 °C in a Sorvall RC6 Plus centrifuge (SS34 rotor) to separate the mitochondria–lysosomal fraction (supernatant) from the nuclei, broken cells, and plasma membrane fragments (pellet). The mitochondria–lysosomal fraction was then loaded on a metrizamide/Percoll gradient and subjected to ultracentrifugation at 68,500 × *g* for 35 min at 4 °C (in a SW41 swinging bucket rotor) to separate light mitochondria and the lysosome fraction from other organelles. This fraction was then further purified to obtain a pure lysosomal population through a second metrizamide/Nycodenz-only discontinuous gradient, where the separation takes place based on the flotation of the organelles. Ultimately the pure lysosomal population was obtained in the pellet form upon centrifugation of the lysosome band from the gradient at 100,000 × *g* for 30 min at 4 °C in a TLA100 rotor to eliminate metrizamide/Nycodenz from the samples. Isolated lysosomes resuspended in 200 μL of 0.25 M sucrose were used to measure ^{3}H-leucine content in lysosomes by scintillation counting and were processed further to determine Lamp1 content by Western blotting using anti-Lamp1 antibody.

Rapid Method for LysoIP. LysoIP from cells was performed according to a published method (13). In brief, ~35×10^6 cells grown in 150 mm × 25 mm dishes were collected in 1 mL of KPBS (136 mM KCl and 10 mM KH_2PO_4; pH 7.25 was adjusted with KOH) and pelleted by centrifuging at 1,000 × *g* for 2 min at 4 °C. The cell pellets were resuspended in 950 μL of buffer, of which 25 μL was saved for whole-cell extract, while the remainder was subjected to homogenization in a Teflon/glass homogenizer with 20 strokes on ice to ensure proper cell membrane disruption. The homogenate was then centrifuged at the above-mentioned speed and conditions to recover cellular organelles, including lysosomes in the supernatant, which was then subjected to incubation with 150 μL of KPBS-prewashed anti-hemagglutinin (HA) magnetic beads (Thermo Fisher Scientific, Waltham, MA) on a gentle rotator shaker for 3 min at 4 °C to capture/immunoprecipitate lysosomes tagged with transmembrane protein 192 (TMEM192)–2×HA. The immunoprecipitates were then gently washed three times with KPBS on a DynaMag Spin Magnet (Thermo Fisher Scientific, Waltham, MA), and the lysosomes were collected in 200 μL of KPBS buffer at the end of the last wash to measure the ^{3}H-leucine amount in lysosomes by scintillation counting and to process further for Western blotting to quantify Lamp1 using anti-Lamp1 antibody. LysoIP was performed in a similar manner from negative control cells expressing TMEM192-2×Flag (see *SI Appendix*, Fig. S3).

Surface Sensing of Translation (SUnSET) Assay/Translation Rate Measurement. The protein synthesis/translation rate in cells was measured using the SUnSET assay, where 90 μM puromycin was added 10 min before harvesting the cells under the different indicated conditions. Puromycin, being the structural analog of tyrosyl-tRNA, was incorporated in the newly synthesizing proteins, which in turn generates puromycin-labeled peptides that can be detected in whole-cell lysates by Western blotting using an anti-puromycin antibody. By using this technique, changes in translation patterns under different conditions can be quantified.

Time-Lapse Microscopy. Cells were plated on glass-bottom dishes (P06G-1.5-20-F, MatTek) in full medium overnight and were then imaged by time-lapse microscopy at 37 °C and 5% CO_2 in a live-cell incubation chamber. LLOMe (300 nM) was added to the medium, and cells were imaged for 1 h at 15-min time intervals, as indicated. For LysoTracker staining experiments, MEFs were incubated with 100 nM LysoTracker Red DND-99 (L7528, Thermo Fisher Scientific, Waltham, MA) for 10 min followed by three PBS washes prior to treatment

with or without 100 nM concanamycin A. Cells were then imaged by confocal microscopy. Fluorescence confocal micrographs were acquired using the Ultraview Vox spinning-disk confocal system (PerkinElmer, Waltham, MA) equipped with a Yokogawa CSU-X1 spinning-disk head and an electron-multiplying charge-coupled device camera (Hamamatsu C9100-13) coupled to a Nikon Ti-E microscope equipped with a CFI Plan Apo VC ×60 oil objective. *Z* stacks (0.5-μm steps) were acquired with a Piezo *z* stack drive controlled by a nano drive (Mad City Lab, Madison, WI).

KO or Knockdown Using CRISPR. CRISPR was performed by cloning small guide RNAs (sgRNA) against *SESTRIN2* and *Depdc5* in the lenti-CRISPRv2 vector backbone, according to Shalem et al. (31), and viruses were generated by transfection into HEK-293T cells. Cell pools were infected with three or four different sgRNA constructs and selected for antibiotic resistance, after which the knockdown efficiency was tested by Western blotting of cell pools using specific antibodies. The most efficient knockdown-bearing cell line was used for further experiments.

The following CRISPR guide sequences were used for knockdowns or KOs: *SESN2* sense, GACTACCTGCGGTTCGCCC; *SESN2* antisense, GGGCGAACCGCAG GTAGTC; *Depdc5* sense, ATTTAGTAAACAGGTCGGCG; *Depdc5* antisense, CGCCGACCTGTTTACTAAATC; control sense, GAAGATGGGCGGGAGTCTTC; control antisense, GAAGACTCCCGCCCATCTTC.

Lamtor1- and *Lamtor2*-KO lines were obtained using CRISPR–Cas9-derived gene editing. pSpCas9(BB)-2A-GFP plasmid was purchased from Addgene (plasmid 48138). Guides targeting *Lamtor1*, *Lamtor2*, or a nongenic region on mouse chromosome 8 (ch8) (32) were cloned into the Cas9 plasmid. ESCs were electroporated with the corresponding plasmid using a Nucleofector 4D (Amaxa, Lonza) and plated onto inactivated feeder MEFs in maintenance medium. After 48 h, transfected cells were selected based on GFP expression by fluorescence-activated cell sorting. GFP-positive cells were plated onto feeder MEFs at clonal density. After ∼10 d, single colonies were picked and expanded for analysis. Successful KO was confirmed by Western blotting. The following CRISPR guide sequences were used: *Lamtor1* (guide 4) sense, CTGCTATAG CAGCGAAAACG; *Lamtor1* (guide 4) antisense, CGTTTTCGCTGCTATAGCAG; *Lamtor2* (guide 4) sense, GCGTCCCAAGGCTTTGACGC; *Lamtor2* (guide 4) antisense, GCGTCAAAGCCTTGGGACGC; ch8 sense, GACATTTCTTTCCCCACTGG; ch8 antisense, CAGTGGGGAAAGAAATGTC.

Western Blotting. Protein concentrations for Western blotting were determined by using the Pierce bicinchoninic acid (BCA) Protein Assay kit (Thermo Fisher Scientific, Waltham, MA). Fifteen micrograms of protein was subjected to 8 to 16% sodium dodecyl-sulfate polyacrylamide gel electrophoresis (SDS-PAGE) in mini polyacrylamide gels after boiling in electrophoresis sample buffer for 5 to 10 min. BenchMark prestained protein ladder (Invitrogen, Carlsbad, CA) was loaded in one of the lanes to determine the molecular weight of proteins. Electrophoresis was performed in a Bio-Rad gel apparatus (Mini-Protean Tetra Vertical Electrophoresis Cell) under a constant voltage of 100 V for 10 min, followed by 160 V for 1 h, after which proteins were transferred from gels to polyvinylidene fluoride (PVDF) membranes using constant voltage (100 V) for 1 h on a Bio-Rad transfer apparatus. Transferred proteins were incubated with 5% BSA in 1× Tris-buffered saline and 0.1% Tween (TBST) and optimized concentrations (0.5 to 2 μg/mL) of designated antibody overnight at 4 °C. Protein levels were visualized by using chemiluminescence (PerkinElmer, Waltham, MA) using horseradish peroxidase (HRP)-conjugated secondary antibodies diluted to 1:1,000 in blocking solution after two 15-min washes with 1× TBST. Quantitative measurements of protein levels were performed using an EPSON image analyzer along with ImageJ software (33).

Statistics. Statistical significance between different samples was determined by the Student's *t* test (TTEST). *P* values ≤ 0.05 are summarized with an asterisk (*), *P* values ≤ 0.01 are summarized with two asterisks (**), *P* values ≤ 0.001 are summarized with three asterisks (***), and *P* values ≤ 0.0001 are summarized with four asterisks (****).

Data Availability. All study data are included in the article and/or supporting information. Reagents generated from this study are available on request, subject to a materials transfer agreement.

ACKNOWLEDGMENTS. We thank members of the M.O., L.W.S.F., and C.B.T. laboratories for helpful discussions. The research was supported by grants from the NIH (RO1GM111350 to M.O. and R01CA201318 and P30CA008748 to C.B.T.).

1. W. Palm, C. B. Thompson, Nutrient acquisition strategies of mammalian cells. *Nature* **546**, 234–242 (2017).
2. S. Sengupta, T. R. Peterson, D. M. Sabatini, Regulation of the mTOR complex 1 pathway by nutrients, growth factors, and stress. *Mol. Cell* **40**, 310–322 (2010).
3. D. H. Kim *et al.*, mTOR interacts with raptor to form a nutrient-sensitive complex that signals to the cell growth machinery. *Cell* **110**, 163–175 (2002).
4. Y. Sancak *et al.*, The Rag GTPases bind raptor and mediate amino acid signaling to mTORC1. *Science* **320**, 1496–1501 (2008).
5. X. Jiang, M. Overholtzer, C. B. Thompson, Autophagy in cellular metabolism and cancer. *J. Clin. Invest.* **125**, 47–54 (2015).
6. R. C. Russell, H. X. Yuan, K. L. Guan, Autophagy regulation by nutrient signaling. *Cell Res.* **24**, 42–57 (2014).
7. N. T. Neff, L. Bourret, P. Miao, J. F. Dice, Degradation of proteins microinjected into IMR-90 human diploid fibroblasts. *J. Cell Biol.* **91**, 184–194 (1981).
8. N. T. Neff, P. A. Ross, J. C. Bartholomew, M. J. Bissell, Leucine in cultured cells: Its metabolism and use as a marker for protein turnover. *Exp. Cell Res.* **106**, 175–183 (1977).
9. D. L. Thiele, P. E. Lipsky, Mechanism of L-leucyl-L-leucine methyl ester-mediated killing of cytotoxic lymphocytes: Dependence on a lysosomal thiol protease, dipeptidyl peptidase I, that is enriched in these cells. *Proc. Natl. Acad. Sci. U.S.A.* **87**, 83–87 (1990).
10. T. O. Berg, E. Strømhaug, T. Løvdal, O. Seglen, T. Berg, Use of glycyl-L-phenylalanine 2-naphthylamide, a lysosome-disrupting cathepsin C substrate, to distinguish between lysosomes and prelysosomal endocytic vacuoles. *Biochem. J.* **300**, 229–236 (1994).
11. S. Aits *et al.*, Sensitive detection of lysosomal membrane permeabilization by lysosomal galectin puncta assay. *Autophagy* **11**, 1408–1424 (2015).
12. B. Storrie, E. A. Madden, Isolation of subcellular organelles. *Methods Enzymol.* **182**, 203–225 (1990).
13. M. Abu-Remaileh *et al.*, Lysosomal metabolomics reveals V-ATPase- and mTOR-dependent regulation of amino acid efflux from lysosomes. *Science* **358**, 807–813 (2017).
14. G. A. Wyant *et al.*, mTORC1 activator SLC38A9 is required to efflux essential amino acids from lysosomes and use protein as a nutrient. *Cell* **171**, 642–654 (2017).
15. C. C. Thoreen *et al.*, An ATP-competitive mammalian target of rapamycin inhibitor reveals rapamycin-resistant functions of mTORC1. *J. Biol. Chem.* **284**, 8023–8032 (2009).
16. L. Bar-Peled *et al.*, A tumor suppressor complex with GAP activity for the Rag GTPases that signal amino acid sufficiency to mTORC1. *Science* **340**, 1100–1106 (2013).
17. R. L. Wolfson *et al.*, Sestrin2 is a leucine sensor for the mTORC1 pathway. *Science* **351**, 43–48 (2016).
18. K. Inoki, Y. Li, T. Zhu, J. Wu, K. L. Guan, TSC2 is phosphorylated and inhibited by Akt and suppresses mTOR signalling. *Nat. Cell Biol.* **4**, 648–657 (2002).
19. Y. Sancak *et al.*, Ragulator-Rag complex targets mTORC1 to the lysosomal surface and is necessary for its activation by amino acids. *Cell* **141**, 290–303 (2010).
20. F. Beaumatin *et al.*, mTORC1 activation requires DRAM-1 by facilitating lysosomal amino acid efflux. *Mol. Cell* **76**, 163–176 (2019).
21. S. Nada *et al.*, The novel lipid raft adaptor p18 controls endosome dynamics by anchoring the MEK-ERK pathway to late endosomes. *EMBO J.* **28**, 477–489 (2009).
22. Y. C. Kim *et al.*, Rag GTPases are cardioprotective by regulating lysosomal function. *Nat. Commun.* **5**, 4241 (2014).
23. R. Milkereit *et al.*, LAPTM4b recruits the LAT1-4F2hc Leu transporter to lysosomes and promotes mTORC1 activation. *Nat. Commun.* **6**, 7250 (2015).
24. P. Nurse, A. Wiemken, Amino acid pools and metabolism during the cell division cycle of arginine-grown *Candida utilis*. *J. Bacteriol.* **117**, 1108–1116 (1974).
25. C. Commisso *et al.*, Macropinocytosis of protein is an amino acid supply route in Ras-transformed cells. *Nature* **497**, 633–637 (2013).
26. W. Palm *et al.*, The utilization of extracellular proteins as nutrients is suppressed by mTORC1. *Cell* **162**, 259–270 (2015).
27. J. Debnath, S. K. Muthuswamy, J. S. Brugge, Morphogenesis and oncogenesis of MCF-10A mammary epithelial acini grown in three-dimensional basement membrane cultures. *Methods* **30**, 256–268 (2003).
28. B. W. Carey, L. W. Finley, J. R. Cross, C. D. Allis, C. B. Thompson, Intracellular α-ketoglutarate maintains the pluripotency of embryonic stem cells. *Nature* **518**, 413–416 (2015).
29. S. Kaushik, A. M. Cuervo, Methods to monitor chaperone-mediated autophagy. *Methods Enzymol.* **452**, 297–324 (2009).
30. U. Bandyopadhyay, S. Kaushik, L. Varticovski, A. M. Cuervo, The chaperone-mediated autophagy receptor organizes in dynamic protein complexes at the lysosomal membrane. *Mol. Cell. Biol.* **28**, 5747–5763 (2008).
31. O. Shalem *et al.*, Genome-scale CRISPR-Cas9 knockout screening in human cells. *Science* **343**, 84–87 (2014).
32. L. E. Dow *et al.*, Inducible in vivo genome editing with CRISPR-Cas9. *Nat. Biotechnol.* **33**, 390–394 (2015).
33. C. A. Schneider, W. S. Rasband, K. W. Eliceiri, NIH Image to ImageJ: 25 years of image analysis. *Nat. Methods* **9**, 671–675 (2012).

CELL BIOLOGY